古 脊 椎 动 物 学 报
VERTEBRATA PALASIATICA

DOI: 10.19615/j.cnki.1000-3118.180302

New material of the Late Miocene *Moschus* (Artiodactyla, Mammalia) from Huade, Nei Mongol, North China

DONG Wei[1,2] LIU Wen-Hui[1,3] ZHANG Li-Min[1] BAI Wei-Peng[1,3] CAI Bao-Quan[4]

(1 *Key Laboratory of Vertebrate Evolution and Human Origins of Chinese Academy of Sciences*, *Institute of Vertebrate Paleontology and Paleoanthropology*, *Chinese Academy of Sciences* Beijing 100044 dongwei@ivpp.ac.cn)
(2 *Center for Excellence in Life and Paleoenvironment* Beijing 100049)
(3 *University of Chinese Academy of Sciences* Beijing 100049)
(4 *Department of History*, *Xiamen University* Xiamen 361005)

Abstract *Moschus grandaevus* was firstly uncovered from the Late Miocene deposits at Ertemte, Olan Chorea, Harr Obo and Hua Ba in or around Huade County in the middle part of Nei Mongol and was described by Schlosser in 1924. The excavations by Sino-Soviet Joint Paleontological Team in 1959 and recent excavations since 2013 at Tuchengzi (Tuchetse), another locality at Huade, accumulated many specimens of the musk deer. The morphology and metric studies show that the musk deer specimens from Tuchengzi are the same as those described by Schlosser and can be included into the same species. *M. grandaevus* ranges from Siberia of Russia to North China, and likely to southern China, in the Late Miocene and Pliocene. The appearance of such folivorous musk deer in the Late Miocene deposits at Tuchengzi indicates that there were forests there during that period. The cladistic analyses show that the fossil species of *Moschus* are closely related to each other and can be grouped together as Moschini or Moschinae. *Micromeryx* is closer to *Moschus* and Cervidae, but the relationship between *Micromeryx* and *Moschus* is more complicated than previously considered; nonetheless *Hispanomeryx* is closer to Bovidae.

Key words Tuchengzi, Huade, Nei Mongol; Late Miocene; Moschidae, *Moschus*

Citation Dong W, Liu W H, Zhang L M et al., in press. New Material of the Late Miocene *Moschus* (Artiodactyla, Mammalia) from Huade, Nei Mongol, North China. Vertebrata PalAsiatica, DOI: 10.19615/j.cnki.1000-3118.180302

1 Introduction

Musk deer is well known for its musk gland which is very famous in Chinese medicine. The extant musk deer refer only to one genus *Moschus*. But for fossil musk deer, it is quite controversial both for their taxonomic composition and phylogenetic relationships (Viret, 1961; Morales et al., 1981; Moyà-Solà, 1986; Janis and Scott, 1987, 1988; Scott and Janis, 1993; McKenna and Bell, 1997; Gentry et al., 1999; Vislobokava and Lavrov, 2009; Sánchez et al., 2010, 2015; Wang et al., 2015; Aiglstorfer et al., 2017). A small and the first true musk deer, *Moschus grandaevus*, was reported by Schlosser in 1924. It is represented by some fragmental

国家自然科学基金(批准号：41372027)资助。
收稿日期：2017-11-26

dentitions and a few limb bones from Ertemte, Olan Chorea, Harr Obo and Hua Ba in Huade County, a northeastern county of Ulanqab Municipality in middle Nei Mongol, North China. The area was firstly explored by Swedish geologist and paleontologist Johan Gunna Andersson and his Chinese collaborators in 1919 and 1920 (Andersson, 1923), then by Schlosser (1924), and later by a Sino-Soviet Joint Expedition Team in 1959 (Zhai, 1963; Qiu, 1979). Many specimens of *M. grandaevus* were collected from a locality at Tuchengzi (Tuchetse) in 1959's excavation. Tuchengzi locality (Google map address: <https://goo.gl/maps/q4JfefaNs2H2>; Baidu map address: <http://j.map.baidu.com/k9M5N>) with Late Miocene deposits is about 16.3 km right south of Ertemte locality. The specimens of the musk deer collected in 1959 were identified but just briefly described (Qiu, 1979). The recent excavations since 2013 at Tuchengzi (Dong et al., 2014, 2016, 2018) enriched the collection of the musk deer. Here we systematically describe the new material of the musk deer collected from Tuchengzi in recent excavations, together with undescribed limb bones collected in 1959, and discuss the phylogenetic and taxonomic relationships of fossil musk deer with other related taxa.

The dental terminology follows Dong (2004), upper teeth are abbreviated in upper case and the lower ones in lower case. The measurement methods follow Heintz (1970). The specimens described are housed at the Institute of Vertebrate Paleontology and Paleoanthropology, Chinese Academy of Sciences, Beijing.

2 Systematic paleontology

Mammalia Linnaeus, 1758
(Clade: Cetartiodactyla Montgelard et al., 1997)
Artiodactyla Owen, 1848
Ruminantia Scopoli, 1777
Pecora Flower, 1883
Cervoidea Simpson, 1931
Moschidae Gray, 1821
Moschinae Zittel, 1893
***Moschus* Linnaeus, 1758**
***Moschus grandaevus* Schlosser, 1924**

1924 *Moschus grandaevus*, Schlosser, p. 89–91
1926 *Moschus grandaevus*, Teilhard de Chardin, p. 40–41
1932 *Moschus grandaevus*, Young, p. 22
1979 *Moschus grandaevus*, Qiu, p. 224–225
1993 *Moschus grandaevus*, Dong and Jiang, p. 119
2014 *Moschus grandaevus*, Dong, p. 24–25

Material Two left maxillary fragments with DP4–M3 (IVPP V 23514.1) and M1–3 (V 23514.2); two right maxillary fragments with M2–3 (V 23514.3) and M2–3 (V 23514.4); eight right mandibular fragments with p3–m3 (V 23515.1), with p3–m3 (V 23515.3), with broken p4 and complete m1–3 (V 23515.4), with complete m1–2 and broken m3 (V 23515.5),

with dp4–m1 (V 23515.7), with m2–3 (V 23515.9), with dp4 (V 23515.10) and with p2–m2 (V 23515.11); three left mandibular fragments with p3–m3 (V 23515.2), with dp4–m2 (V 23515.6) and with m2–3 (V 23515.8). A proximal fragment of right metacarpus (V 23516.3); two distal fragments of metacarpus (V 23516.1–2); two left astragalus (V 23516.4–5); two proximal middle phalanges (V 23516.6–7); three intermediate middle phalanges (V 23516.8–10); a distal middle phalange (V 23516.11).

Description The maxillary dentition available only ranges from DP4 to M3 (see Table 1 for measurements). The DP4 (5.78 mm×5.92 mm) is composed of four simple main cusps in two distinct lobes (Fig. 1A), the buccal main cusps are higher than the lingual ones. The entostyle is present and moderate, but other accessory elements such as precingulum, entocingulum, postcingulum, spur, neocrista, etc. are absent. The maxillary molars are morphologically similar to each other and relatively simple, the accessory elements such as precingulum, postcingulum, neocrista, entostyle (basal pillar), etc. are absent. But the molars are characterized by the presence of metaconule spur which is not evident on M1, slightly evident on M2 and very clear on M3. The evidence of the spur is probably related to the degree of wearing. It is very evident on the molars unworn or slightly worn (Fig. 1A, D), but might disappear on the crowns very worn, especially on M1. The entocingulum is also present on the molars but poorly developed.

The mandibular dentition available ranges from the second premolar to the last molar, as well as a last deciduous tooth (Fig. 2). The measurements of lower teeth are listed in Table 2 and comparison in Table 3.

Table 1 Measurements of upper cheek teeth of *Moschus grandaevus* and comparison (mm)

	V 23514.1	V 23514.2	V 23514.3	V 23514.4	A	B	C	D	E	F	G	H
P2 L						6.3	7	5.3				4.3–5.5
P2 W						4.5	4.5	4				2.1–3
P3 L						5.8		6.2				5–6.5
P3 W						5.3		6				4.1–5.3
P4 L						5.8	5	6.1				5.1–5.9
P4 W						5.8	5	6				4.1–6.1
P2–4 L						15.6						16.1–18.5
M1 L	6.32	6.18			7	6.4	7	(8.8)			9.82	6.2–7.3
M1 W	6.26	6.42			7	7.2	5	(8.7)			7.84	5.1–7.8
M1 H	5.58	3.88					4.5				8.64	3.5–6.3
M2 L	6.82	6.68	6.88	7.06	7	7.5	7	(9.7)				6.1–9
M2 W	7.1	6.76	7.78	6.86	7	7.4	5	(8.6)				6.2–8.3
M2 H	6.46	5.42	7.72	4.34			4.5					4.3–7.2
M3 L	6.5	7.12	7.76	6.98	7	7.2	8					8.5–9.5
M3 W	7.02	6.78	7.82	7.28	7	7.2	7.5					6.1–8.3
M3 H	6.38	6.52	5.12	5.12	6		4.5					4.1–7.1
M1–3 L	20.62	20.72				20.2			26	23		21.5–24.7
P2–M3 L						35.5		44	43	41		

Note: A. *Moschus grandaevus* from Huade (Schlosser, 1924; Teilhard de Chardin, 1926); B. *M. grandaevus* from Yushe (Vislobokova and Lavrov, 2009); C. *M. primaevus* (Teilhard de Chardin, 1926); D. *M. moschiferus pekinensis* (Young, 1932; values in brackets are measured on the plates); E. *M. moschiferus plicodon* (Colbert and Hooijer, 1953); F. *M. chrysogaster sifanicus* (Colbert and Hooijer, 1953); G. *M. moschiferus moschiferus* (Dong and Jiang, 1993); H. extant *M. m. moschiferus*, specimens from Asia and housed at Laboratoire d'Anatomie Comparé de Paris and measured by the first author.

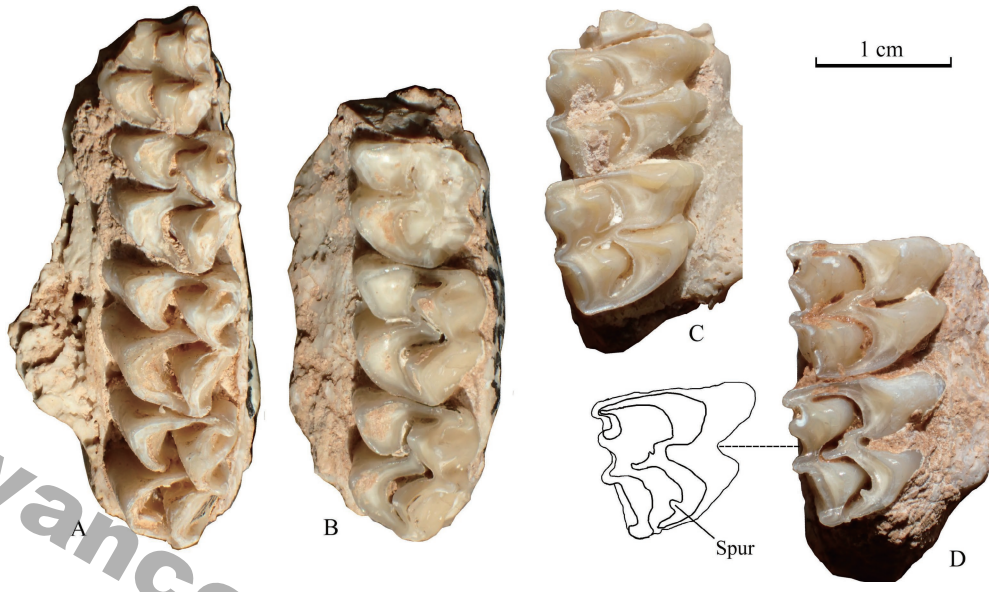

Fig. 1 Occlusal view of maxillary fragments with upper cheek teeth of *Moschus grandaevus* from Tuchengzi locality
A. DP4–M3 (IVPP V 23514.1); B. M1–3 (V 23514.2); C. M2–3 (V 23514.3); D. M2–3 (V 23514.4)

Table 2 Measurements of lower cheek teeth of *Moschus grandaevus* from Tuchengzi locality (mm)

	V 23515.1	-.2	-.3	-.4	-.5	-.6	-.7	-.8	-.9	-.10	-.11
p2 L	4.32		4.02								4.02
p2 W	2.36		2.32								2.38
p2 H											3.16
p3 L	5.46	6.68	5.96								5.02
p3 W	3.12	3.02	3.04								3.02
p3 H	3.9	3.96	3.02								3.66
p4 L	6.38	6.58	6.42								5.72
p4W	3.72	4.36	3.48								3.54
p4 H	5.02	3.86	2.86								3.68
dp4 L						8.12	8.22			8.92	
dp4 W						3.68	3.58			3.54	
p2–4 L	15.32		15.86								15.02
m1 L	7.16	6.18	6.66	6.92	7.42	6.72	6.48				6.72
m1 W	4.48	4.76	4.22	4.28	4.8	4.32	4.22				4.72
m1 H	4.5		5.22	4.26	2.42	4.78	4.44				3.62
m2 L	6.78	7.52	7.62	6.64	7.46	7.26		7.44	7.56		7.12
m2 W	4.92	4.62	4.72	4.62	5.12	4.48		4.28	4.34		4.94
m2 H	5.62	5.02	2.88	5.22	2.76	4.78		4.12	4.32		3.62
m3 L	10.12	10.28	10.44	10.52				9.78	9.42		
m3 W	4.78	4.74	5.02	4.52				4.12	4.32		
m3 H	5.56	5.16	2.58	4.96				4.14	4.32		
m1–3 L	24.92	23.06	22.64	22.82							
p2–m3 L	39.34		37.76								

Note: the measurments of p2 on IVPP V 23515.1 and V 23515.3 are based on the broken roots in mandibular fragments.

The p2 is composed of two main cusps. Paraflexid and talonid basin are not evident, trigonid basin and entoflexid are present and opened lingually, the hypoflexid is absent. The p3

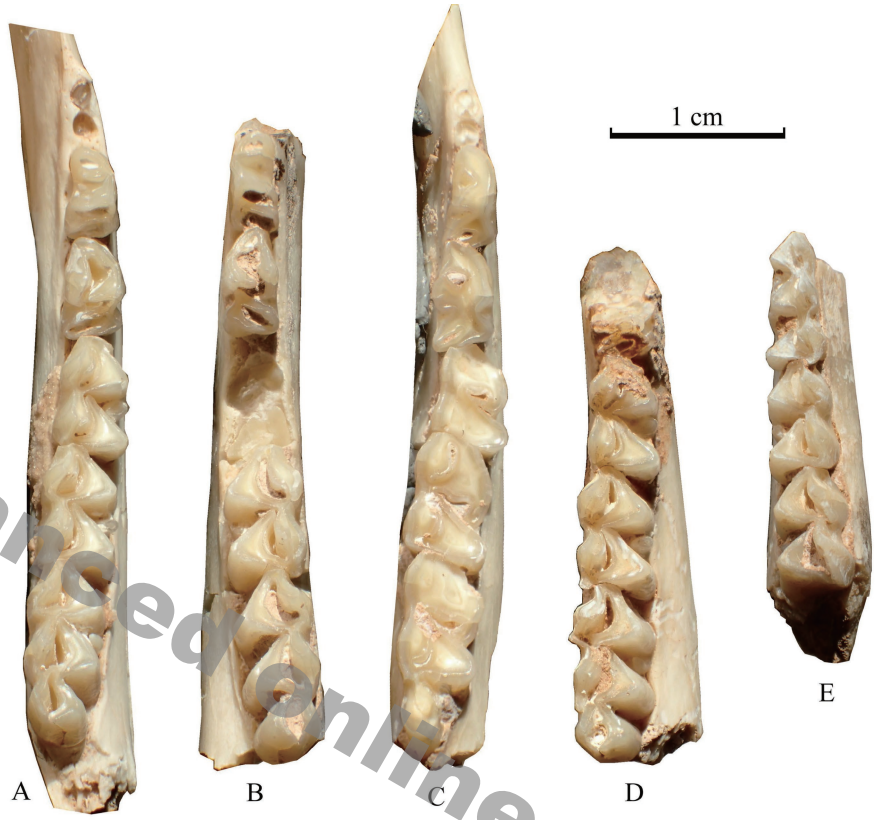

Fig. 2 Occlusal view of lower cheek teeth of *Moschus grandaevus* from Tuchengzi locality
A, C. two right mandibular fragments with p3−m3 (IVPP V 23515.1, V 23515.3);
B, E. two left mandibular fragments with p3−m3 (V 23515.2) and dp4–m2 (V 23515.6) respectively;
D. a right mandibular fragment with broken p4 and complete m1−3 (V 23515.4)

is composed of two main cusps and some minor cusps (Fig. 2A−C). Paraflexid, trigonid basin, entoflexid and talonid basin are all present and opened lingually, the hypoflexid is also present but poorly developed. The p4 is characterized by the molarization. The premetacristid extends forward and reaches parastylid, so that the paraflexid and trigonid basin are completely closed. The paraconid is reduced and enclosed by extended premetacristid. It makes the anterior lobe of the p4 analogous to that of the lower molars (Fig. 2A−C). The entoflexid and hypoflexid are well developed and open. The entoconid extends lingually and backwards so that it reaches entostylid to close the talonid basin. The posterior lobe of the p4 is also similar to that of the lower molar, but its size is much smaller than the anterior one.

The m1 is composed of four selenodont main cusps, the *Palaeomeryx* fold is evidently absent. The precingulid is present, but at the superior part of the crown. The postcingulid and ectocingulid are all absent. The ectostylid is present and developed, but quite isolated (Fig. 2A, C−E). The m2 (Fig. 2A−E) morphology resembles the m1. The m3 is composed of three lobes, and the anterior two lobes resemble those of m1 and m2, but the third lobe is composed of a developed hypoconulid and a small entoconulid (Fig. 2A−D).

Table 3 Comparison of lower cheek teeth among different *Moschus* (mm)

V 23515	N	Min	Max	M	A	B	C	D	E	F	G
p2 L	3	4.02	4.32	4.12	5	5.2		5	(4.2–5.0)	4.04–4.7	4
p2 W	3	2.32	2.38	2.35		2.4				2.12–3.2	
p2 H	1	3.16	3.16	3.16	3					3.62–3.62	
p3 L	4	5.02	6.68	5.78		5.7	6.2	6.5	(5.3–6.5)	5.7–6.1	5.5
p3 W	4	3.02	3.12	3.05		3.5				3.6–4	
p3 H	4	3.02	3.96	3.64						4.94–5.74	
p4 L	4	5.72	6.58	6.28	6.5	6.2	6.8–7.1	6.3	(6.9–7.0)	6.92–7.44	6.5
p4W	4	3.48	4.36	3.78		3.8	4.1–4.2			3.9–4.68	
p4 H	4	2.86	5.02	3.86	6					2.32–6.54	
dp4 L	3	8.12	8.92	8.42				9	(9.7)	9.18–10.38	
dp4 W	3	3.54	3.68	3.60						4.22–4.34	
p2–4 L	3	15.02	15.86	15.40		15.2			17–17.5	16.7–19.22	
m1 L	8	6.18	7.42	6.78	7	6.8	7.3–7.8	7	(7.3–8.4)	7.64–8.74	8
m1 W	8	4.22	4.8	4.48	4.5	4.9	4.6–5.1			5.02–5.38	
m1 H	7	2.42	5.22	4.18	5					2.3–8.04	
m2 L	9	6.64	7.62	7.27	8	7.2	7.3–8.2	7.5	(9.0–9.2)	8.74–10.24	8
m2 W	9	4.28	5.12	4.67	5	5.3	4.7–5.5			5.42–6.06	
m2 H	9	2.76	5.62	4.26	6					3.08–9.5	
m3 L	6	9.42	10.52	10.09	10	10.2	7.9–11.1	11	(12.7–13.6)	11.38–12.48	12
m3 W	6	4.12	5.02	4.58		5.0	4.8–5.3			5.56–6.12	
m3 H	6	2.58	5.56	4.45						4.9–7.5	
m1-3 L	4	22.64	24.92	23.36	~25	22.2	26.8–26.9		30–31	28.7–29.68	
p2–m3 L	2	37.76	39.34	38.55	~40	37.2		44	46–48	45.4–46.3	46

Note: A. *Moschus grandaevus* from Huade (Schlosser, 1924); B. *M. grandaevus* from Yushe (Vislobokova and Lavrov, 2009); C. *M. grandaevus* from Olkhon, Russia (Vislobokova and Lavrov, 2009); D. *M. primaevus* (Teilhard de Chardin, 1926); E. *M. moschiferus pekinensis* (Young, 1932; values in brackets are measured on the plates); F. *M. moschiferus moschiferus* (Dong and Jiang, 1993); G. *M. moschiferus* (Teilhard de Chardin, 1926). N. number; Min. minimum; Max. maximum; M. Mean.

The dp4 is completely molarized (Fig. 2E). It is composed of three lobes, the width of the lobe increases from the first to the last.

The enamel on both upper and lower dentitions is generally smooth.

Eleven pieces of limb bones of a very small sized artiodactyls (V 23516.1–11) are recognized as of *M. grandaevus* (Fig. 3). They are dimensionally very small (see Table 4 for measurements) among all artiodactyls materials from Tuchengzi locality and proportionally match well with the teeth described above.

The metacarpus is represented by three fragments, a proximal one (V 23516.3) and two distal ones (V 23516.1–2). The proximal view is nearly triangle (Fig. 3Aa), with the medial side the shortest, the posterior or palm side curves inwards. The distal part of the metacarpus shows a nutrient foramen (medullary foramina) on the anterior side (Fig. 3Bb) as well as posterior side (Fig. 3Bc). The metacarpal gully is not evident on both anterior (dorsal) and posterior (palm) sides, the fusion of metacarpus III and IV is quite complete.

The astragalus or talus is represented by two complete specimens (V 23516.4–5), both left ones (Fig. 3C–D). The proximal trochlea (trochlea tali) is well developed. The crest for articulation with fibula and calcaneus is more developed, wider and higher, than that for articulation with tibia. The distal part of the talus, or head of the talus (caput tali), forms a second trochlea as in all artiodactyls, although less developed than the proximal trochlea.

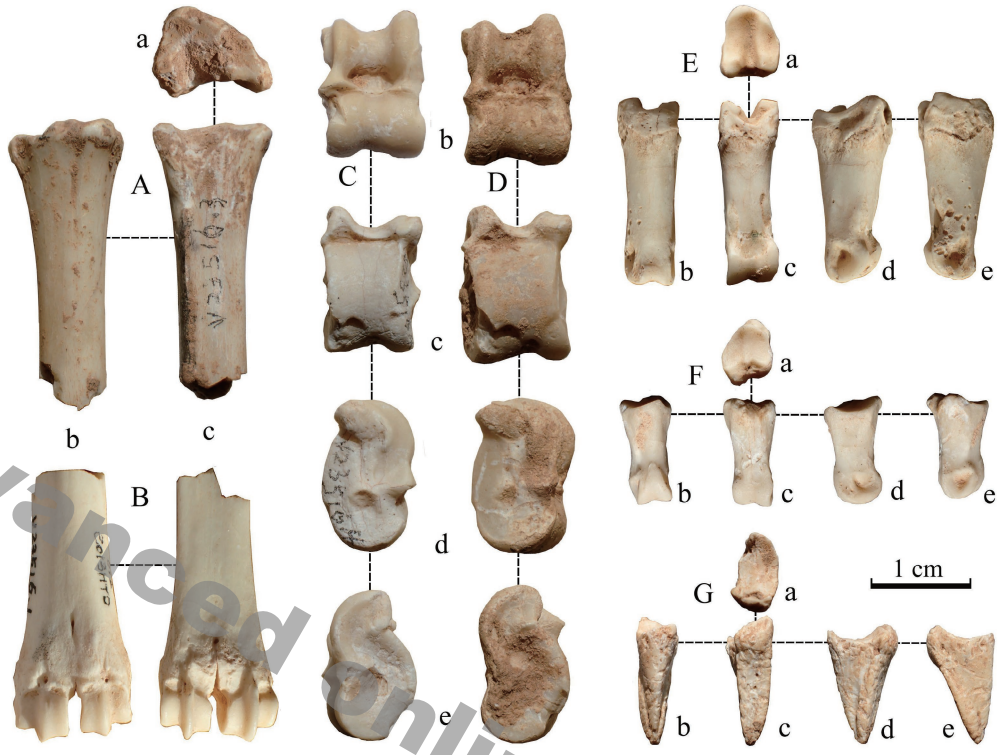

Fig. 3 Limb bones of *Moschus grandaevus* from Tuchengzi collected in recent years
A. a proximal fragment of right metacarpus (IVPP V 23516.3); B. a distal fragment of metacarpus (V 23516.1); C–D. two left astragalus (V 23516.4–5); E. a proximal middle phalange (V 23516.7); F. an intermediate middle phalange (V 23516.10); G. a distal middle phalange (V 23516.11). a. proximal view; b. dorsal view; c. palm/ventral view; d. medial view; e. lateral view

Table 4 Measurements of limb bones of *Moschus grandaevus* from Tuchengzi collected in recent years and comparison (mm)

	Metacarpus				Astragalus				
	V 23516.1	V 23516.2	V 23516.3	D	V 23516.4	V 23516.5	A	B	C
PAPD			9.96		7.28	8.32			
PTD			12.38	17	9.88	10.82		9.2–10	
MAPD	5.12		6.12						
MTD	7.24		7.06						
Length					15	15.82	17	17.1–17.2	18
DAPD	7.38	6.96			7.82	7.96			
DTD	11.62	11.04		16.5	9.82	10.02	11		11

	Phalanx I			Phalanx II			Phalanx III	
	V 23516.6	V 23516.7	A	V 23516.8	V 23516.9	V 23516.10	V 23516.11	B
PAPD	7.76	8.06		6.88	7.36	6.38	7.68	
PTD	6.54	6.56		5.72	5.58	4.14	4.22	
Length	17.52	18.72	20	12.66	11.26	10.52	13.04	12.5–14.5
DAPD	4.72	5.14		5.52	5.52	4.72		
DTD	5.14	5.16	5	4.08	4.34	4.78		

Note: A. *Moschus grandaevus* from Huade (Schlosser, 1924); B. *M. grandaevus* from Olkhon, Russia (Vislobokova and Lavrov, 2009); C. *M. primaevus* (Teilhard de Chardin, 1926); D. *M. moschiferus pekinensis* (Young, 1932). PAPD. proximal anteroposterior diameter; PTD. proximal transversal diameter; MAPD. middle anteroposterior diameter; MTD. middle transversal diameter; DAPD. distal anteroposterior diameter; DTD. distal transversal diameter.

The proximal middle phalange (Fig. 3E) is represented by two specimens (V 23516.6–7), the intermediate middle phalange (Fig. 3F) is represented by three specimens (V 23516.8–10), and the distal middle phalange only one specimen (V 23516.11). It is not evident if they are the third or fourth, of the anterior or posterior limbs. They are very typical of artiodactyls, and the only peculiar trait is that the distal middle phalange is significantly narrow (Fig. 3G).

Many limb bones of *M. grandaevus* from the same locality under one same number IVPP V 5631.3 were collected by the Sino-Soviet Joint Expedition in 1959 and mentioned by Qiu (1979), but not yet described. Some representatives of these old specimens (Fig. 4), i.e. the parts not present in the new materials depicted above, are described as follow and the measurements are given in Table 5.

Two incomplete scapula specimens are available (Fig. 4A–B). Their dorsal margin is broken and missing. The lateral view of the scapula is rather narrow. The scapula spine (spina scapulae) is developed but its outer margin also incompletely preserved. The infraspinous fossa (fossa infraspinata) is much larger than that of supraspinous (fossa supraspinata) which seems very limited. The acromion is not evident, but the tuberculum supraglenoidale is well developed. In medial view, the subscapula fossa (fossa subscapularis) is generally flat and slightly concave.

Table 5 Measurements of limb bones of *Moschus grandaevus* from Tuchengzi collected in 1959's excavations and comparison (mm)

	Scapula		Humerus					
	V 5631.3	V 5631.3	V 5631.3	V 5631.3	A	B	C	D
PAPD	10.22	10.76						
PTD	12.68	12.92						18
MAPD	5.82	6.42	6.96	8.46				
MTD	8.32	8.62	7.96	7.78				
Length	>30	>33						123
DAPD			12.64	11.62				
DTD			14.92	15.02	14	14.0–14.4	17.5–18	20.5

	Radius			Femur	Tibia				
	V 5631.3	C	D	V 5631.1	V 5631.3	A	B	C	D
PAPD				12.44					
PTD		12.0–12.4	17	24.82					30
MAPD				11.96	7.22				
MTD				11.02	9.96				
Length					>51				198
DAPD	9.58				10.22				
DTD	12.72	15.5	10		15.62	14	13.5–15.7	15.5–17	19

	Calcaneus				Metatarsus				
	V 5631.3	V 5631.3	A	C	V 5631.3	A	B	C	D
PAPD	8.6	9.04			13.24				
PTD	6.32	6.3			11.78		11.1–12.6		13
MAPD	9.52	10.18			9.38				
MTD	9.94	9.96			8.18				
Length	33.14	32.56	38		>30		107.5		132
DAPD	12.24	12.76							
DTD	4.02	4.62		11		8.5	14.5–14.7	15	19

See footnote of Table 4 for abbreviations and labels.

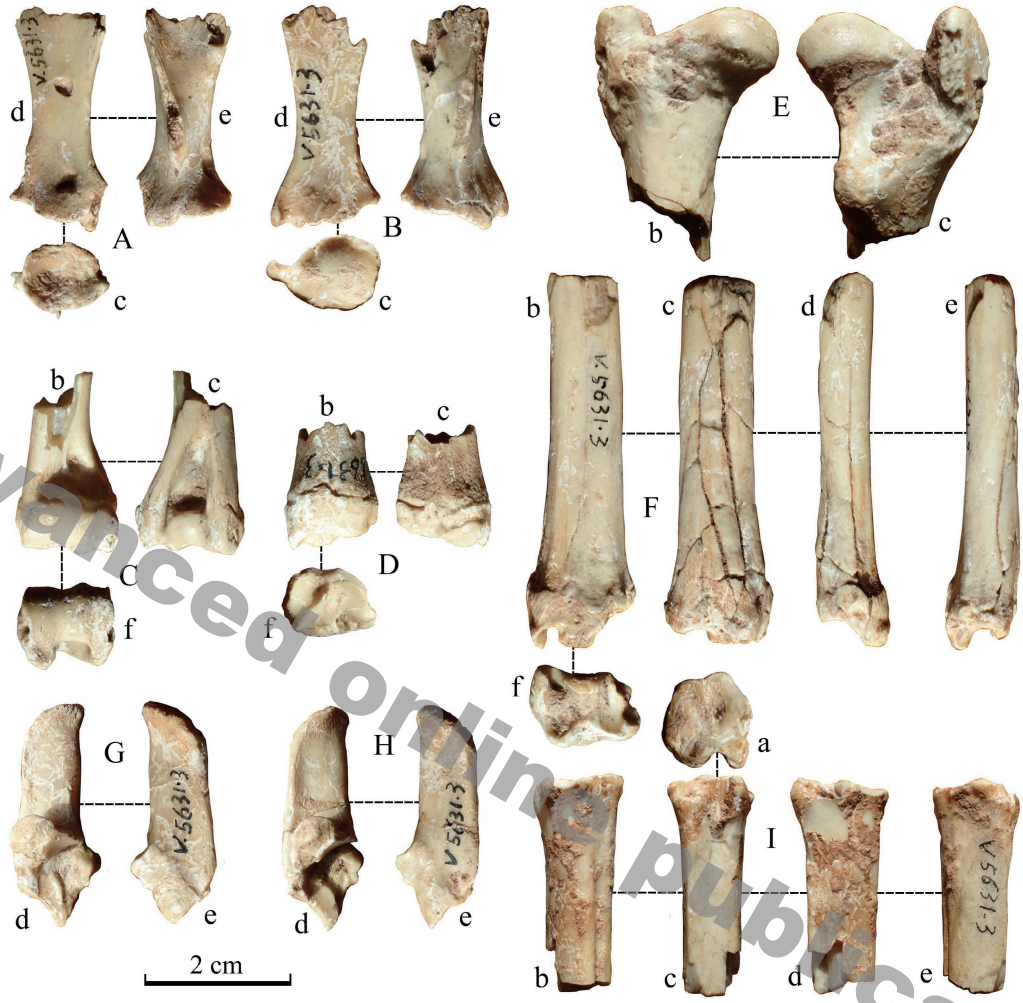

Fig. 4 Limb bones of *Moschus grandaevus* (IVPP V 5631.3) from Tuchengzi collected in 1959. A–B. incomplete right and left scapula respectively; C–D. distal fragment of left humerus and radius respectively; E. a proximal fragment of right femur; F. a distal fragment of left tibia; G–H. two complete left calcaneus; I. a proximal fragment of left metatarsus. a. proximal view; b. dorsal/anterior view; c. ventral/posterior view; d. medial view; e. lateral view; f. distal view

The humerus available is two distal fragments. In anterior view (Fig. 4Cb), the humerus condyle is composed of humerus trochlea on the medial side and humerus capitulum with a sagittal crest on the lateral side. The radius fossa is developed above humerus condyle. In posterior view (Fig. 4Cc), both medial and lateral epicondyles are well developed, with a developed olecranon fossa in between. In distal view (Fig. 4Cf), the medial and lateral epicondyles are divided by a trochlea gully, and both epicondyles are nearly equal sized.

The radius available is a distal end of a left one (Fig. 4D). The transversal crest is evident on the posterior side. A moderate trochlea is developed on the distal end for articulation with carpus.

The femur available is a proximal end of a right one (Fig. 4E). The femur head (caput ossis femoris) is eminent and protrudes medially. The major trochanter is also eminent and protrudes posteriorly. They are aligned at the same level and separated from each other by femur neck and trochanter fossa. The minor trochanter is well developed.

The tibia available is three distal fragments. The anterior side is concave longitudinally (Fig. 4Fb), and the posterior one convex (Fig. 4Fc). The medial malleolus is well developed (Fig. 4Fd) and that of the lateral one is moderate (Fig. 4Fe). The distal surface for articulation with talus is composed of two fossae or gullies with medial one longer than lateral one (Fig. 4Ff).

The calcaneus available is two complete left specimens (Fig. 4G–H). The calcaneal tuber is half semicircular in both medial and lateral views. The calcaneal body is plank-like. The sustentaculum tali is well developed. The processus coracoideus is eminent. The base of calcaneus, or distal end, is also developed into a coracoid processus.

No complete metatarsus is available. The metatarsus identifiable is three proximal fragments, the distal fragments are not distinct from those of metacarpus. The proximal view of metatarsus is polygonal, with anterior-posterior diameter close to that of medial-lateral one (Fig. 4Ia). The metatarsal gully is evident on the anterior side and eminent on the posterior side (Fig. 4Ib, c). The medial and lateral sides are nearly flat (Fig. 4Id, e).

Comparison Tuchengzi specimens are nearly the same as those of *Moschus grandaevus* from Ertemte and Olan Chorea established by Schlosser (1924) both metrically (Tables 1, 3–5) and morphologically, and they can be grouped into the same taxon. Vislobokova and Lavrov (2009) discussed some specimens of *M. grandaevus* from Yushe in northern China. The specimens are metrically very close to those of Tuchengzi (Tables 1, 3) and can also be included into the same species. Vislobokova and Lavrov (2009) described, meanwhile, some other specimens of *M. grandaevus* from Olkhon Island in Baikal and Taralyk-Cher in Tuva, Russia. The dimensions of Olkhon specimens are generally very close to, except a few parts slightly larger than, those of Tuchengzi specimens (Tables 3–5). The cingula are absent on upper molars, *Palaeomeryx* fold is absent but ectostylid is present on lower molars, anterior lobe of p4 is well molarized, in both Tuchengzi and Olkhon specimens. The differences appear on limb bones: the proximal crest of talus for articulation with fibula and calcaneus is more developed and the shaft of metapodials is more slender in Olkhon specimens.

There are only two fossil species of *Moschus*: *M. grandaevus* and *M. primaevus*. Compared with *M. primaevus* from the Early Pliocene deposits in Huiteng River (Chiton-gol) area established by Teilhard de Chardin (1926), the dentitions of both forms share the following traits: brachyodont, the similar measurements (Tables 1, 3–5), presence of the spur on metaconule of upper molars, molarization of the anterior lobe of p4. But the most significant morphological difference is that the *Palaeomeryx* fold is evidently present in Huiteng River specimens and absent in those from Ertemte and Tuchengzi.

There are six extant species of *Moschus* in China: *M. moschiferus*, *M. anhuiensis*, *M. berezovskii*, *M. fuscus*, *M. chrysogaster* and *M. leucogaster* (Wang, 2003). But only *M.*

moschiferus, with three subspecies, is present in geological time: *M. moschiferus moschiferus*, *M. moschiferus pekinensis* and *M. moschiferus plicodon*. Compared with the *M. moschiferus pekinensis* from the Middle Pleistocene Localities 1 and 3 of Zhoukoudian described by Young (1932) and Pei (1936), Tuchengzi specimens are characterized by lower tooth crown and smaller dimensions (Tables 1, 3–5). The metaconule spur on upper cheek teeth and ectostylid on lower molars are present in both Zhoukoudian and Tuchengzi specimens, but more developed in Zhoukoudian specimens. And the metaconule spur is absent in extant *M. moschiferus* (Young, 1932).

The *M. moschiferus plicodon* from the Middle Pleistocene deposits of Yanjinggou (Yenchingkou) established by Colbert and Hooijer (1953) differs from Tuchengzi specimens by higher tooth crown, presence of precingulid on lower molars, as well as larger dimensions (Tables 1, 3). Nevertheless, both forms have molarized anterior lobe of p4, presence of ectostylid and absence of *Palaeomeryx* fold on lower molars.

Compared with *M. moschiferus moschiferus* from the Late Pleistocene deposits in Xianren Cave at Ji'an in Jilin Province (Dong and Jiang, 1993), Tuchengzi specimens share with Ji'an specimens the same characters such as molarized anterior lobe of p4, presence of ectostylid and absence of *Palaeomeryx* fold on lower molars. But the crown height and other dimensions of Ji'an specimens are evidently larger than those of Tuchengzi specimens (Tables 1, 3).

Compared with the extant musk deer such as that mentioned by Teilhard de Chardin (1926), that from Asia and housed at Laboratoire d'Anatomie Comparé de Paris, as well as *Moschus chrysogaster sifanicus* of Sichuan (Colbert and Hooijer, 1953), Tuchengzi specimens are metrically smaller (Tables 1, 3).

Three maxillary fragments and more than three dozens of mandibular fragments of *Moschus* sp. were mentioned by Han (1985) in her preliminary report on the artiodactyls from type locality of *Lufengpithecus* at Shihuiba, Lufeng, Yunnan Province in southern China. The specimens were not described but briefly indicated as generally close to *M. grandaevus* of Ertemte and different from *M. primaevus* by absence of *Palaeomeryx* fold. The specimens are unfortunately unavailable for comparison. But another *Moschus* sp. from Yuanmou *Lufengpithecus* localities near Lufeng with similar horizon is probably the same species as that from Shihuiba (Pan et al., 2006). Compared with Tuchengzi specimens, Yuanmou specimens are metrically larger, and morphologically simpler. The metaconule spur and ectostylid are present in Tuchengzi specimens but absent in Yuanmou specimens. However, the *Palaeomeryx* fold is absent in both forms.

3 Discussion

3.1 Geographic and geological ranges of fossil musk deer

Moschus grandaevus (Schlosser, 1924) is the first fossil musk deer reported in China, the specimens were from Ertemte, Olan Chorea, Harr Obo and Hua Ba in or around Huade County

in the middle part of Nei Mongol. The species was discovered again during 1959's Sino-Soviet expedition but at Tuchengzi locality (Qiu, 1979), also from the Late Miocene in Huade County. It was later uncovered from the Pliocene deposits in Yushe Basin in Shanxi Province (Tedford et al., 1991; Vislobokova and Lavrov, 2009). As mentioned above, *Moschus* sp. from the Late Miocene deposits of Lufeng and Yuanmou in Yunnan Province in southern China shows some similarities to *M. grandaevus* of Huade, and might be the same species, or closely related species.

The second fossil musk deer, *M. primaevus* (Teilhard de Chardin, 1926), was from Huiteng River area southwest of Xilinhot in eastern Nei Mongol (Li et al., 2003). The species has not yet been found elsewhere. The presence of *Palaeomeryx* fold on the lower molars of the species distinguishes it from other musk deer and it was considered as *Lagomeryx primaevus* (Vislobokova, 1990; Vislobokova and Lavrov, 2009).

In the Middle Pleistocene, two fossil subspecies of *M. moschiferus* were reported. *M. moschiferus pekinensis* was found from the Middle Pleistocene Locality 1 and Locality 3 of Zhoukoudian in Beijing (Young, 1932; Pei, 1936), then from the Early Pleistocene Locality 18 of Zhoukoudian (Teilhard de Chardin, 1940), and later from the Late Pleistocene Xiaogushan Paleolithic site in Liaoning Province of northeastern China (Zhang et al., 1985). *M. moschiferus plicodon* was found from the Middle Pleistocene of Yanjinggou (Yenchingkou) (Colbert and Hooijer, 1953), and later from the Early Pleistocene Longgupo site (Huang et al., 1991), both sites are in Chongqing Municipality of central China. *M. moschiferus*, or *M. moschiferus moschiferus* from Ji'an in Jilin Province in northeastern China (Dong and Jiang, 1993) is a fossil representative of extant *M. m. moschiferus*. It indicates that the subspecies appeared as early as the Late Pleistocene in northeastern China.

Micromeryx is another fossil genus of Moschidae reported in China (Lee and Wu, 1978; Qiu et al., 1981; Wang et al., 2015). Two species, *Micromeryx* cf. *M. flourensianus* from the Middle Miocene Nanyu Quarry, Gansu Province and *Micromeryx* sp. (IVPP V 18969) from the Middle Miocene Lengshuigou in Shaanxi Province, were recently confirmed and described (Wang et al., 2015). If the fragmental specimens of putative *Micromeryx* sp. from locality DM 16 of Damiao (as early as MN1 or MN2) in Nei Mongol reported by Zhang et al. (2011) can be confirmed for its taxonomic status, it would be the earliest Moschidae from China. Two other *Micromeryx* species, *Micromeryx* sp. (IVPP V 3208 and V 3208.1) from the Middle Miocene Lengshuigou in Shaanxi Province (Lee and Wu, 1978) and *Micromeryx* sp. (IVPP V 6023 and V 6023.1-2) from Lierbao Quarry, Qinghai Province, the Middle Miocene Xianshuihe Formation, (Qiu et al., 1981), were revised as *Hispanomeryx* sp. 1 and *Hispanomeryx* sp. 2 respectively and described recently (Wang et al., 2015).

3.2 Paleo-ecological consideration

The brachyodont dentitions of *Moschus grandaevus* imply that it was a browser. Its proportionally long limbs indicate the musk deer was a good jumper. The extant musk deer

is partially arboreal (Sheng et al., 1992) that extends its browsing range and helps it escaping from large-sized predators. The narrow and sharp hooves (Fig. 3) and lightly built body size of *M. grandaevus* suggest it could also be partially arboreal. Its habitat might be a mixture of shrubs and large trees. It could hide in the shrubs, jump on to the branches of shrubs, and jump further on to the branches of large trees for wider range of leaves or getting rid of predators.

3.3 Phylogenetic relationship of musk deer

Hispanomeryx is a controversial genus of Moschidae. Its taxonomic and systematic status was referred either to Moschidae (e.g. Morales et al., 1981; McKenna and Bell, 1997; Vislobokava and Lavrov, 2009) or to Bovoidea (e.g. Moyà-Solà, 1986; Gentry et al., 1999). Likewise, the Moschidae was considered either closely related to Cervidae (e.g. Janis and Scott, 1987, 1988; Scott and Janis, 1993; Su et al., 1999; Hernández Fernández and Vrba, 2005; Aiglstorfer et al., 2017) or closely related to Bovidae (e.g. Sánchez et al., 2010, 2015; DeMiguel et al., 2014). Here we try to test the phylogenetic relationship of fossil musk deer with cervids, bovids and other related taxa (see Table 6 for data matrix) by cladistic analyses with PAUP4.0a (Build 159) programmed by Swofford (2002).

Eighteen fossil taxa with as more available characters as possible, including hypothetic ancestor, all species of *Moschus*, two *Micromeryx*, three *Hispanomeryx*, two cervids and two bovids, a palaeomerycid, a tragulid, were selected for cladistic analyses with the data source as follow: *Dorcabune* cf. *D. progressus* (Pan et al., 2006); *Palaeomeryx tricornis* (Qiu et al., 1985); *Moschus grandaevus*; *M. primaevus* (Teilhard de Chardin, 1926); *Moschus* sp. (from Yuanmou, Yunnan; Pan et al., 2006); *M. moschiferus pekinensis* (Young, 1932); *M. m. plicodon* (Colbert and Hooijer, 1953); *M. m. moschiferus* (Dong and Jiang, 1993); *Micromeryx* cf. *M. flourensianus* (Wang et al., 2015); *Micromeryx azanzae* (Sánchez and Morales, 2008); *Hispanomeryx* sp. 1 (from Lengshuigou, Shaanxi; Wang et al., 2015); *H. andrewsi* (Sánchez et al., 2011); *H. daamsi* (Sánchez et al., 2010); *Hydropotes inermis* (Young, 1932); *Cervavitus shanxius* (Dong and Hu, 1994; Dong et al., 2018); *Gazella sinensis* (Dong et al., 2013) and *Leptobos* (*Smertiobos*) *crassus* (Dong, 2008). The characters chosen and their states are as follows:

1. Frontal appendages: 0. absent; 1. antlers; 2. ossicones; 3. horns.
2. Upper canines: 0. tusk-like; 1. small; 2. absent.
3. Crown height of cheek teeth: 0. low; 1. moderate; 2. high.
4. Number of main cusps on P2: 0. four; 1. three; 2. two.
5. Lingual cusp fold(s) on P2: 0. absent; 1. weak (present but not developed, just one fold); 2. strong (developed and with two or more folds).
6. Number of main cusps on P3: 0. four; 1. three; 2. two.
7. Lingual cusp fold(s) on P3: 0. absent; 1. weak (present but not developed, just one fold); 2. strong (developed and with two or more folds).
8. Number of main cusps on P4: 0. four; 1. three; 2. two.
9. Lingual cusp fold(s) on P4: 0. absent; 1. weak (present but not developed, just one fold); 2. strong (developed and with two or more folds).

10. Pattern of lingual main cusps on upper molars and buccal main cusps on lower ones: 0. nearly conical; 1. selenodont; 2. nearly triangular.
11. Pattern of buccal main cusps on upper molars and lingual main cusps on lower ones: 0. somewhat conical; 1. selenodont; 2. nearly cylindrical; 3. nearly semi-circular.
12. Precingulum on upper molars: 0. absent; 1. weak; 2. developed.
13. Entocingulum on upper molars: 0. absent; 1. weak; 2. developed.
14. Entostyle (basal pillar) on upper molars: 0. absent; 1. moderate; 2. developed; 3. very developed.
15. Neocrista on upper molars: 0. absent; 1. moderate; 2. developed.
16. Metaconule fold on upper molars: 0. absent; 1. present.
17. Metaconule spur on upper molars: 0. absent; 1. moderate; 2. developed.
18. Undulation of buccal main cusp wall of upper molars: 0. smooth; 1. moderate; 2. strong.
19. Anterior extension of premetacristid on p4: 0. absent; 1. moderate; 2. strong.
20. Size of paraconid on p4: 0. moderately developed; 1. present but reduced.
21. Opening of trigonid basin (lingual valley between paraconid and metaconid) on p4: 0. widely open; 1. half open; 2. closed by anteriorly extension of premetacristid.
22. Paraflexid state on p4: 0. present and open; 1. present but closed by anterior extension of premetacristid; 2. disappeared.
23. Opening of talonid basin (lingual valley between entoconid and entostylid) on p4: 0. widely open; 1. half open; 2. closed.
24. Cristid obliqua on the p4: 0. present; 1. absent.
25. Lower premolar vs. lower molar row length: 0. nearly equally long; 1. reduced premolar row.
26. *Palaeomeryx* fold: 0. developed; 1. present but weak; 2. absent.
27. Crown ratio of the lower molars: 0. relatively shorter and broader; 1. relatively narrower and elongated.
28. Precingulid on lower molars: 0. absent; 1. moderate; 2. hypertrophied.
29. Orientation of the prehypocristid on lower molars: 0. straight and pointing to the center of the teeth; 1. lingually-turned and fused with the pre-entocristid.
30. Ectocingulid on lower molars: 0. absent; 1. present but weak; 2. developed.
31. Ectostylid (basal pillar) on lower molars: 0. absent; 1. present but weak; 2. developed; 3. hypertrophied.
32. Hypotalonid basin of the m3: 0. distally open; 1. distally closed.
33. Entoconulid vs. hypoconulid on m3: 0. the lengths of entoconulid and hypoconulid nearly the same; 1. hypoconulid evidently longer than entoconulid.
34. Morphology of the articular facet for the semilunate in the radius: 0. without lateral notch; 1. with lateral notch.
35. Morphology of the tuber calcanei: 0. short and broad; 1. transversally compressed and dorsoplantarly elongated.
36. General morphology of the astragalus: 0. slender and elongated; 1. short and wide.
37. Morphology of the lateral condyle in the distal trochlea of the astragalus: 0. very inclined and sporting a triangular and well marked proximal notch; 1. vertical or slightly inclined, without proximal notch.
38. Morphology of metatarsal shaft: 0. very slender; 1. less slender.
39. Metatarsal gully: 0. little developed; 1. moderately developed; 2. very developed.

All characters in Table 6 are unordered and equally weighted. The heuristic search found 101 most parsimonious trees and among which 18 optimal trees were retained. The strict and

semistrict consensus trees based on all optimal trees are the same. The Adams consensus tree (Fig. 5) is nearly the same as the strict and semistrict consensus trees with the only difference that *Dorcabune* cf. *D. progressus* and *Palaeomeryx tricornis* derives together from the first node in strict and semistrict consensus trees rather than from the second node as in Adams consensus tree. As the cladogram illustrates, three Neogene musk deer species, *Moschus grandaevus*, *M. primaevus* and *Moschus* sp. (from Yunnan), form a monophyly; and three Quaternary musk deer subspecies, *M. moschiferus pekinensis*, *M. m. plicodon* and *M. m. moschiferus*, form another monophyly. They are sister groups and form a further monophyly which can be grouped as Moschini or even as a subfamily Moschinae because *Micromeryx* does not form a monophyly with *Moschus* and could not be placed in Moschinae. *Micromeryx* is closer to *Moschus* and cervids (*Cervavitus shanxius* and *Hydropotes inermis*) than to *Hispanomeryx*. And the latter is closer to *Gazella sinensis* than to cervids and musk deer.

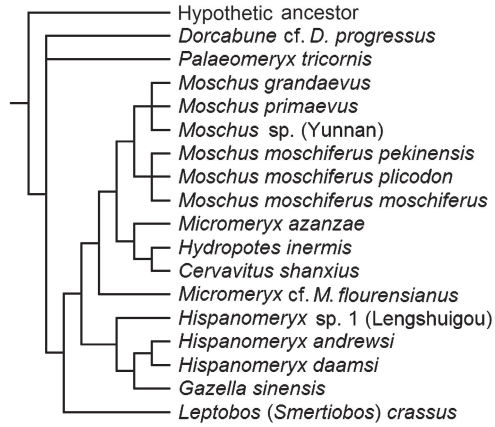

Fig. 5 Adams consensus tree of 18 optimal trees found by heuristic search based on data matrix in Table 6

Based on the fossil evidences and Fig. 5, *Moschus* might derive from the stem including *Micromeryx*. And *Moschus* might form a clade of its own. Cervidae might also derive from the stem including *Micromeryx* or its closely related clade. While *Hispanomeryx* might derive from a bovids dominated clade.

Table 6 Data matrix for cladistic analyses

Taxa								
Hypothetic ancestor	00000	00000	00000	00000	00000	00000	00000	0000
Dorcabune cf. *D. progressus*	0?0??	??100	00101	00100	00200	20000	110??	????
Palaeomeryx tricornis	2002?	1?200	01101	11100	00000	00101	110??	????
Moschus grandaevus	000??	????1	10100	02121	21100	20100	21000	0000
Moschus primaevus	00011	??221	12111	12121	21100	10100	210??	????
Moschus sp. (Yunnan)	0?0??	????1	10100	0?1??	?????	20100	210??	????
Moschus moschiferus pekinensis	00111	22201	10000	00121	21100	20100	210??	????
Moschus moschiferus plicodon	00111	12201	10000	00121	21100	20200	210??	????
Moschus moschiferus moschiferus	001??	????1	10000	00121	21100	20100	21000	000?
Micromeryx cf. *M. flourensianus*	0?0??	????1	1????	???11	1020?	20100	100??	????
Micromeryx azanzae	0?0??	??201	10000	02111	10101	20101	210??	????
Hispanomeryx sp. 1 (Lengshuigou)	0?1??	11202	20000	001??	????1	21000	210??	????
Hispanomeryx andrewsi	0?1??	????2	30000	00121	22211	21010	101??	11??
Hispanomeryx daamsi	0?110	20202	30000	01121	22211	21110	10111	1102
Hydropotes inermis	001??	??211	10000	01111	12100	20101	110??	????
Cervavitus shanxius	11101	02221	11212	12110	10100	20101	210??	????
Gazella sinensis	322??	??202	30000	00111	12201	21010	011??	????
Leptobos (*Smertiobos*) *crassus*	32220	20202	20030	00200	00200	20000	310??	1011

This result in Fig. 5 is based on available material, mostly dentitions and a few post-cranial skeletons, and all characters are unordered and equally weighted. The result may vary if some characters are ordered and weighted, or with the accumulation of new and more complete specimens.

4 Conclusions

The musk deer specimens from Tuchengzi are the same as those of *Moschus grandaevus* from Ertemte, Olan Chorea, Harr Obo and Hua Ba in or around Huade County in the middle part of Nei Mongol, and can be included into the same species. It ranges from Siberia of Russia to North China, and likely to southern China, in the Late Miocene and Pliocene.

The appearance of folivorous and partially arboreal musk deer in the Late Miocene deposits at Tuchengzi indicates that there were forests there during that period.

The fossil species of *Moschus* are closely related to each other and can be grouped together as Moschini or Moschinae. *Micromeryx* is closer to *Moschus* and Cervidae than to *Hispanomeryx*, but the relationship between *Micromeryx* and *Moschus* is more complicated than previously considered; nonetheless *Hispanomeryx* is closer to Bovidae. The systematic status of *Micromeryx* and *Hispanomeryx* remain to be further investigated with more complete materials.

Acknowledgments The authors would like to thank the Office for Protection of Paleontological Fossils of Nei Mongol Autonomous Region and the Land and Resources Bureau of Huade County for cooperation during the excavations. The authors are grateful to the reviewers for their comments and suggestions to improve this manuscript.

内蒙古化德土城子地点晚中新世麝科化石新材料

董　为[1,2]　刘文晖[1,3]　张立民[1]　白炜鹏[1,3]　蔡保全[4]

(1 中国科学院脊椎动物演化与人类起源重点实验室，中国科学院古脊椎动物与古人类研究所 北京 100044)

(2 生物演化与环境卓越创新中心 北京 100049)

(2 中国科学院大学 北京 100049)

(3 厦门大学历史系 厦门 361005)

摘要：Schlosser (1924)记述了最初发现于内蒙古化德境内或附近的二登图、敖兰卓蕾、哈尔敖包及华坝的古麝(*Moschus grandaevus*)。1959年中苏古生物考察队在化德的另一个地点土城子采集到不少古麝化石。2013年以来作者在土城子进行的野外发掘积累了更多的古麝化石标本。土城子标本在形态和测量数据方面和二登图等地点的古麝非常接近，可以归入同一种。根据现有资料归纳，古麝的地理分布范围自俄罗斯的西伯利亚到华北，很可能延

伸到华南；其地质时代分布范围为晚中新世–上新世。食叶型古麝在土城子晚中新世地层中的出现说明当时土城子一带有森林环境。支序分析显示麝属(*Moschus*)化石种相互之间的系统关系非常近，可以归并为麝族(Moschini)或麝亚科(Moschinae); *Micromeryx*更接近麝属和鹿科，它与麝属之间的关系比以前认为的复杂，而*Hispanomeryx*更接近牛科。

关键词：内蒙古化德土城子，晚中新世，麝科，古麝

References

Aiglstorfer M, Costeur L, Mennecart B et al., 2017. *Micromeryx*? *eiselei* – A new moschid species from Steinheim am Albuch, Germany, and the first comprehensive description of moschid cranial material from the Miocene of Central Europe. PLoS ONE, 12(10): e0185679

Andersson J G, 1923. Essays on the Cenozoic of northern China. Mem Geol Surv China, Ser A, 3: 1–152

Colbert E H, Hooijer D A, 1953. Pleistocene mammals from the limestone fissures of Szechwan, China. Bull Am Mus Nat Hist, 102(1): 1–134

DeMiguel D, Azanza B, Morales J, 2014. Key innovations in ruminant evolution: a paleontological perspective. Integr Zool, 9: 412–433

Dong W, 2004. The dental morphological characters and evolution of Cervidae. Acta Anthrop Sin, 23(supp): 286–295

Dong W, 2008. Nouveau matériel de *Leptobos (Smertiobos) crassus* (Artiodactyla, Mammalia) du Pléistocène inférieur à Renzidong (Chine de l'est). Geobios, 41(3): 355–364

Dong W, 2014. Brief report on 2009-2010's investigation on Neogene fossil localities in Huade, Nei Mongol. In: Dong W ed. Proceedings of the Fourteenth Annual Meeting of the Chinese Society of Vertebrate Paleontology. Beijing: China Ocean Press. 19–28

Dong W, Hu C K, 1994. The Late Miocene Cervidae from Hounao, Yushe Basin, Shanxi. Vert PalAsiat, 32(3): 209–227

Dong W, Jiang P, 1993. The Late Pleistocene Cervoidea (Artiodactyla) from Xianren Cave, Ji'an, Jilin. Vert PalAsiat, 31(2): 117–131

Dong W, Liu J Y, Fang Y S, 2013. The large mammals from Tuozidong (eastern China) and the Early Pleistocene environmental availability for early human settlements. Quatern Int, 295: 73–82

Dong W, Cai B Q, Zhang L M et al., 2014. Preliminary report on 2013's test excavation at Tuchengzi fossil locality in Huade, Nei Mongol. In: Dong W ed. Proceedings of the Fourteenth Annual Meeting of the Chinese Society of Vertebrate Paleontology. Beijing: China Ocean Press. 29–36

Dong W, Wang S L, Liu W H et al., 2016. Preliminary report on 2014–2015's excavations at Tuchengzi fossil locality in Huade, Nei Mongol. In: Dong W ed. Proceedings of the Fifteenth Annual Meeting of the Chinese Society of Vertebrate Paleontology. Beijing: China Ocean Press. 53–68

Dong W, Liu W H, Zhang L M et al., 2018. New materials of Cervidae (Artiodactyla, Mammalia) from Tuchengzi of Huade, Nei Mongol, North China. Vert PalAsiat, doi: 10.19615/j.cnki.1000-3118.170823

Gentry A W, Rössner G E, Heizmann E P J, 1999. Suborder Ruminantia. In: Rössner G E, Heissig K eds. The Miocene Land Mammals of Europe. Munich: Verlag Dr. Friedrich Pfeil. 225–258

Han D F, 1985. The Artiodactyla of *Ramapithecus* site, Lufeng, Yunnan. Acta Anthrop Sin, 4(1): 44–54

Heintz E, 1970. Les Cervides Villafranchiens de France et d'Espagne. Mém Mus Natl Hist Nat, 22(1): 1–303

Hernández Fernández M, Vrba E S, 2005. A complete estimate of the phylogenetic relationships in Ruminantia: a dated species-level supertree of the extant ruminants. Biol Rev, 80(2): 269–302

Huang W B, Fang Q R et al., 1991. Wushan Hominid Site. Beijing: China Ocean Press. 1–201

Janis C M, Scott K M, 1987. The Interrelationships of higher ruminant families, with special emphasis on the members of the Cervoidea. Am Mus Novit, 2893: 1–85

Janis C M, Scott K M, 1988. The phylogeny of the Ruminantia (Artiodactyla, Mammalia). In: Benton M J ed. The Phylogeny and Classification of the Tetrapods, Volume 2: Mammals, Systematics Association Special Volume No. 35B. Oxford: Clarendon Press. 273–282

Lee Y Q, Wu W Y, 1978. Miocene Artiodactyla of Lintung and Lantian. Prof Pap Stratigr Palaeont, 7: 127–135

Li Q, Wang X M, Qiu Z D, 2003. Pliocene mammalian fauna of Gaotege in Nei Mongol (Inner Mongolia), China. Vert PalAsiat, 41(2): 104–114

McKenna M C, Bell S K, 1997. Classification of Mammals Above the Species Level. New York: Columbia University Press. 1–640

Morales J, Moyà-Solà S, Soria D, 1981. Presencia de la famila Moschidae (Artiodactyla, Mammalia) en el Vallesiense de España: *Hispanomeryx duriensis* novo gen. nova sp. Estud Geol, 37(5-6): 467–475

Moyà-Solà S, 1986. El genero *Hispanomeryx* Morales et al. (1981): position filogenética y systematica. Su contribucion al conocimiento de la evolucion de los Pecora (Artiodactyla, Mammalia). Paleont Evol, 20: 267–287

Pan Y R, Liu J H, Dong W, 2006. Artiodactyla. In: Qi G Q, Dong W eds. *Lufengpithecus hudienensis* Site. Beijing: Science Press. 195–228

Pei W C, 1936. On the mammalian remains from Locality 3 at Choukoutien. Palaeont Sin, Ser C, 7(5): 1–108

Qiu Z D, 1979. Some mammalian fossils from the Pliocene of Inner Mongolia and Gansu (Kansu). Vert PalAsiat, 17(3): 222–235

Qiu Z D, Li C K Wang S J, 1981. Miocene mammalian fossils from Xining Basin, Qinghai. Vert PalAsiat, 19(2): 156–173

Qiu Z X, Yan D F, Jia H, 1985. Preliminary observations on the newly found skeletons of *Palaeomeryx* from Shanwang, Shandong. Vert PalAsiat, 23(3): 173–195

Sánchez I M, Morales J, 2008. *Micromeryx azanzae* sp. nov. (Ruminantia: Moschidae) from the Middle-Upper Miocene of Spain, and the first description of the cranium of *Micromeryx*. J Vert Paleont, 28(3): 873–885

Sánchez I M, Domingo M S, Morales J, 2010. The genus *Hispanomeryx* (Mammalia, Ruminantia, Moschidae) and its bearing on musk deer phylogeny and systematic. Palaeontology, 53(5): 1023–1047

Sánchez I M, Demiguel D, Quiralt V et al., 2011. The first known Asian *Hispanomeryx* (Mammalia, Ruminantia, Moschidae). J Vert Paleont, 31(6): 1397–1403

Sánchez I M, Cantalapiedra J L, Ríos M et al., 2015. Systematics and evolution of the Miocene three-horned palaeomerycid ruminants (Mammalia, Cetartiodactyla). PLoS ONE, 10(12): e0143034

Schlosser M, 1924. Tertiary vertebrates from Mongolia. Palaeont Sin, Ser C, 1(1): 1–132

Scott K M, Janis C M, 1993. Relationships of the Ruminantia (Artiodactyla) and analysis of the characters used in ruminant taxonomy. In: Szalay F S, Novacek M J, McKenna M C eds. Mammal Phylogeny: Placentals. New York: Springer-Verlag. 282–302

Sheng H L et al., 1992. The Deer in China. Shanghai: East China Normal University Press. 1–305

Su B, Wang Y X, Lan H et al., 1999. Phylogenetic study of complete cytochrome b genes in musk deer (genus *Moschus*) using museum samples. Mol Phylogenet Evol, 12(3): 241–249

Swofford D L, 2002. PAUP*. Phylogenetic Analysis Using Parsimony (*and Other Methods). Version 4. Sinauer Associates, Sunderland, Massachusetts

Tedford R H, Flynn L J, Qiu Z X et al., 1991. Yushe Basin, China: paleomagnetically calibrated mammalian biostratigraphic standard for the Late Neogene of eastern Asia. J Vert Paleont, 11(4): 519–526

Teilhard de Chardin P, 1926. Description de mammifères Tertiaires de Chine et de Mongolie. Ann Paléont, 15(1): 1–52

Teilhard de Chardin P, 1940. The fossils from locality 18 near Peking. Palaeont Sin, New Ser C, 9: 1–100

Viret J, 1961. Artiodactyla. In: Piveteau J ed. Traité de Paléontologie VI, vol. 1. Paris: Masson et Cie. 1038–1084

Vislobokova I A, 1990. On the basic patterns of historical development and classification of Ruminantia. Paleont Zh, 4: 3–14

Vislobokova I A, Lavrov A V, 2009. The earliest musk deer of the genus *Moschus* and their significance in clarifying of evolution and relationships of the family Moschidae. Paleont J, 43: 326–338

Wang S Q, Shi Q Q, Hui Z H et al., 2015. Diversity of Moschidae (Ruminantia, Artiodactyla, Mammalia) in the Middle Miocene of China. Paleont Res, 19(2): 143–155

Wang Y X, 2003. A Complete Checklist of Mammal Species in China—A Taxonomic and Geographic Reference. Beijing: China Forestry Publishing House. 1–394

Young C C, 1932. On the Artiodactyla from the *Sinanthropus* Site at Choukoutien. Palaeont Sin, Ser C, 8(2): 1–158

Zhai R J, 1963. Additional note on *Sinohippus zitteli*. Vert PalAsiat, 7(2): 168–172

Zhang Z H, Fu R Y, Chen B G et al., 1985. A preliminary report on the excavation of Paleolithic site at Xiaogushan of Haicheng, Liaoning Province. Acta Anthrop Sin, 4: 70–79

Zhang Z Q, Wang L H, Kaakinen A et al., 2011. Miocene mammalian faunal succession from Damiao, central Nei Mongol and the environmental changes. Quatern Sci, 31: 608–613